LAWRENCE
LIVERMORE
NATIONAL
LABORATORY

UCRL-CONF-153584

Effects of Nonlinear Absorption in BK7 and Color Glasses at 355 nm

J. J. Adams, T. McCarville, J. Bruere, J. McElroy, and J. Peterson

November 12, 2003

SPIE Boulder Damage Symposium XXXV – Annual Symposium on Optical Materials for High Power Lasers, Boulder, Colorado, September 22-24, 2003

Updated October 14, 2003

Effects of Nonlinear Absorption in BK7 and Color Glasses at 355 nm

John J. Adams, Tom McCarville, Justin Bruere, Jim McElroy, John Peterson
Lawrence Livermore National Laboratory
P.O. Box 808, L-592, Livermore, CA 94551
(925) 422-4663, adams29@llnl.gov

ABSTRACT

We have demonstrated a simple experimental technique that can be used to measure the nonlinear absorption coefficients in glasses. We determine BK7, UG1, and UG11 glasses to have linear absorption coefficients of 0.0217 ± 10% cm^{-1}, 1.7 ± 10% cm^{-1}, and 0.82 ± 10% cm^{-1}, respectively, two-photon absorption cross-sections of 0.025 ± 20% cm/GW, 0.035 ± 20% cm/GW, and 0.047 ± 20% cm/GW, respectively, excited-state absorption cross-sections of $8.0x10^{-18}$ ± 20% cm^2, $2.8x10^{-16}$ ± 20% cm^2, and $5x10^{-17}$ ± 20% cm^2, respectively, and solarization coefficients of $8.5x10^{-20}$ ± 20% cm^2, $2.5x10^{-18}$ ± 20% cm^2, and $1.3x10^{-19}$ ± 20% cm^2, respectively. For our application, nonlinear effects in 10-cm of BK7 are small (≤ 2%) for 355-nm fluences < 0.2 J/cm^2 for flat-top pulses. However, nonlinear effects are noticeable for 355-nm fluences at 0.8 J/cm^2. In particular, we determine a 20% increase in the instantaneous absorption from linear, a solarization rate of 4% per 100 shots, and a 10% temporal droop introduced in the pulse, for 355-nm flat-top pulses at a fluence of 0.8 J/cm^2. For 0.5-cm of UG1 absorbing glass the non-linear absorption has a similar effect as that from 10-cm of BK7 on the pulse shape; however, the effects in UG11 are much smaller.

Keywords: nonlinear absorption, BK7, solarization, color glasses, ultra-violet absorption, cross-sections

1. INTRODUCTION

1.1 Application

The ability to predict the change in transmission due to two-photon absorption, excited-state absorption, and solarization induced by UV laser light in BK7 and color glasses is of interest since these glasses are used in a variety of optical applications. Our particular interest is how these nonlinear effects impact the performance of the full-aperture backscatter diagnostic (FABS) used on the National Ignition Facility (NIF) located at the Lawrence Livermore National Laboratory (LLNL). The FABS diagnostic measures the integrated energy per pulse and the pulse's temporal wave form. A schematic is shown in Figure 1. Pulses of UV light in the 1 – 3 ns range are directed into the FABS diagnostic after passing through BK7, UG1, and UG11 glass. The BK7 window is 10-cm thick and the UG filters are ~0.5-cm thick. Fluences up to 1 J/cm^2 are incident on the BK7 window as shown in Figure 1. Previous work has shown that fluences this high will induce two-photon absorption, excited-state absorption, and solarization.[1] This paper describes a technique that accounts for the transmission change and temporal distortion of the pulse shape due to non-linear effects.

1.2 General Approach

The approach to evaluating non-linear absorption and solarization induced by 355 nm light in BK7 and UG glasses has 4 parts. First, we describe the linear and non-linear absorption equation. The equation is simplified for numerical analysis by making several reasonable assumptions. Second, nonlinear absorption and solarization are induced in 2-cm thick BK7 and 0.3-cm thick UG1 and UG11 glass samples using 6.8 ns pulses and 3.5 ns pulses of 355 nm light. The absorption changes in the glass samples were experimentally measured on a pulse-by-pulse basis for fluences in the range of 0.2 – 0.8 J/cm^2. Third, the absorption cross-sections for each glass were extracted from the data by fitting the finite element solution of the nonlinear absorption equation to the measured transmission data. Fourth, with the cross-sections determined the nonlinear absorption equation is used to calculate the change in transmission and pulse shape for the FABS application.

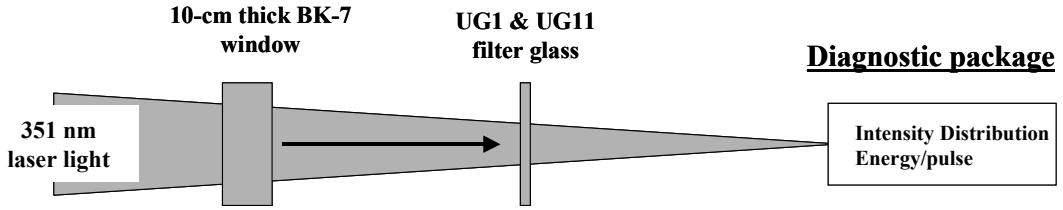

Figure 1: The FABS diagnostic package measures the integrated energy and temporal waveform of UV pulses after they pass through a BK7 window and UG filter glass.

2. SOLVING THE NONLINEAR ABSORPTION EQUATION

2.1 Nonlinear absorption equation

The fractional intensity loss per unit distance of a pulse propagating through an absorptive medium can be expressed as

$$\frac{1}{I}\frac{\partial I(x,\ t)}{\partial x} = -(\underbrace{\alpha}_{\text{Linear}} + \underbrace{\beta I + \sigma_{esa} n_e}_{\text{Nonlinear}} + \overbrace{\sigma_{cc} n_{cc}}^{\text{Slow}}) \qquad (1)$$

where α = linear absorption coefficient (cm^{-1})
β = two-photon absorption cross-section $(cm\text{-}GW)^{-1}$
σ_{esa} = excited-state absorption cross-section (cm^2)
σ_{cc} = color center absorption cross-section (cm^2)
n_e = conduction electron density (cm^{-3})
n_{cc} = color center density (cm^{-3})

Equation (1) contains both linear and nonlinear terms as shown. The coefficient α describes linear absorption. The non-linear terms are illustrated schematically in Figure 2. When the energy of two absorbed photons exceeds the band-gap, a valence electron can be promoted into the conduction band, leaving behind a hole. This two-photon absorption (2PA) is

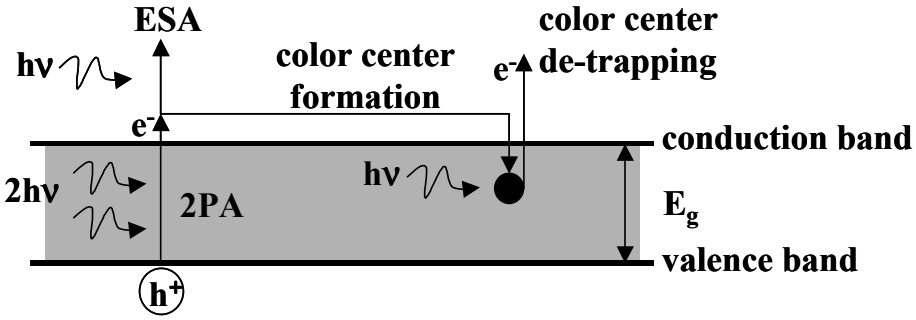

Figure 2: Schematic illustrating the non-linear absorption processes described in equation (1).

represented by the term βI in equation (1). The conduction electrons may interact with single photons and be promoted to excited states. Excited-state absorption (ESA) is represented by the term $\sigma_{esa} n_e$ in equation (1). The majority of

conduction electrons re-combine with holes, but some are trapped by impurities or other defects to form color centers. The formation of color centers is represented by the term $\sigma_{cc}n_{cc}$ in equation (1) (i.e. solarization). There are a number of possible color center species,[2] and each species will have a different density and photon interaction cross-section. In general, the solarization term should be written as a sum over species, but here we represent it as a single term for simplicity. An electron trapped at a color-center can interact with a single photon and be removed or "de-trapped" from the defect, which eventually leads to solarization saturation. The objective of this work is to evaluate the material constants β, σ_{esa}, and σ_{cc}.

The terms in equation (1) evolve on two very different time scales. The conduction electron density accumulates rapidly with absorption interactions, whereas color-center density accumulates comparatively slowly because electrons must migrate a distance in order to encounter a trap. The time scale difference allows us to calculate the conduction electron build-up separately from color-center accumulation.

2.2 Solving for the conduction electron density, n_e

Equation (1) requires expressions for the conduction electron density n_e and color-center density n_{cc}. A simple expression for the conduction electron density is possible if the electron-hole recombination time is long compared to the pulse length. Luminescence lifetime measured for pulsed-irradiated samples show the time for electron-hole recombination is long (>100 ns) compared to the nanosecond scale pulse lengths of interest for this application.[3] In this case, the conduction electron density accumulated during a pulse is simply

$$\mathbf{n_e = \frac{\beta}{2h\nu} \int_{pulse} I^2 dt} \tag{2}$$

This integral is taken over a single pulse, and the conduction electron density is assumed to fall to zero between pulses. This assumption is reasonable as long as the time between pulses is long compared to the electron-hole recombination time. Luminescence lifetime measurements show the recombination time is short (< 1 ms) compared to the duration between our pulses.

For consecutive pulses, equation (2) will change little from pulse to pulse. But its value can change over many pulses as color centers form and the spatial absorption changes. The conduction electron density accumulated per pulse approaches a constant value as solarization approaches saturation.

2.3 Solving for the color center density, n_{cc}

The rate equation for the density of each color center species is given by

$$\mathbf{\frac{\partial n_{cc}(x,t)}{\partial N} = n_e P_{cc}\left(1 - \frac{n_{cc}}{N_T}\right) - \sigma_{dt} n_{cc} \frac{\int_{pulse} I dt}{h\nu}} \tag{3}$$

where N is the number of pulses. The source term is n_eP_{cc}, where P_{cc} is the probability a conduction electron will form a color center, and in general $P_{cc} << 1$. The ratio $\frac{n_{cc}}{N_T}$ represents the limit imposed by a finite trap site density N_T. The third term in equation (3) represents the probability a color-center will be destroyed by interaction with a photon.[4]

If the electron density changes slowly (i.e. $n_e \approx$ constant) from pulse N to N+ΔN pulses, equation (3) can be integrated for the change in color center density during ΔN pulses:

$$\Delta n_{cc} = \frac{P_{cc} n_e}{C}\left(\exp(-CN) - \exp(-C(N+\Delta N)\right) \tag{4}$$

where the constant C is

$$C = \frac{P_{cc} n_e}{N_T} + \sigma_{dt} \frac{\int_{pulse} I dt}{h\nu}(1 - P_{cc}) . \tag{5}$$

Equation (4) allows the effect of solarization to be integrated over many pulses, avoiding pulse-by-pulse numerical integration. This expression applies to each color center species, but discriminating between the affect each species has on the data is generally not straightforward. Some researchers have measured radiation emissions to study the different species, but a simple solution applies for the limiting case of small number of pulses.

2.4 The nonlinear absorption equation for small number of pulses

At the initial onset of solarization, equation (4) simplifies to

$$n_{cc} \approx n_e P_{cc} N_{pulse} \tag{6}$$

where N has been set to zero and N_{pulse} represents the number of accumulated pulses. Using equation (6), the nonlinear absorption equation (1) becomes

$$-\frac{1}{I}\frac{\partial I(x,t)}{\partial x} = \alpha + \beta I + \sigma_{esa} n_e + (P_{cc}\sigma_{cc}) n_e N_{pulse} \tag{7}$$

Equation (7) is linear with number of pulses, and $(P_{cc}\sigma_{cc})n_e$ is the absorption increase per pulse. The absorption increase per pulse from solarization is the cumulative effect of multiple color center species. But at the onset the cumulative effect of all species is conveniently expressed by a single lumped coefficient. For the FABS application, evaluating this limiting case is adequate. With continued pulses the role of various color center species evolves as species saturate at different rates, and equation (6) eventually breaks down.

2.5 Numerical solution

A finite element solution of equation (7) is employed to determine the transmission of an arbitrary pulse waveform through a sample of arbitrary thickness. We re-write equation (7) in finite-element form by dividing each laser pulse into M flat top pulses (see Figure 5) of constant fluence F_i;

$$\left(\frac{\Delta F}{F}\right)_i = \Delta x\left[\alpha + \frac{\beta F_i}{\Delta t} + \sigma_{esa}(n_e)_i + (P_{cc}\sigma_{cc}) n_e (N_{pulse} + \Delta N_{pulse})\right], \tag{8}$$

$$\text{where } (n_e)_i = \frac{\beta}{2h\nu}\sum_1^i \frac{F_i^2}{\Delta t}, \tag{9}$$

$$\text{and } n_e = \frac{\beta}{2h\nu}\sum_1^5 \frac{F_i^2}{\Delta t} \tag{10}$$

For a gaussian pulse, five sub-pulses are adequate to conserve energy within a few percent. The conduction electron density n_e at location x is held constant over a number of pulses ΔN_{pulse}, until the fluence changes by a few percent due to solarization. Then the value of n_e is updated for the next increment of pulses.

The fluence dependence of each term is clearly visible in equation (8). For a fixed pulse length, two-photon absorption scales with fluence F, while excited-state absorption and solarization scale as F^2.

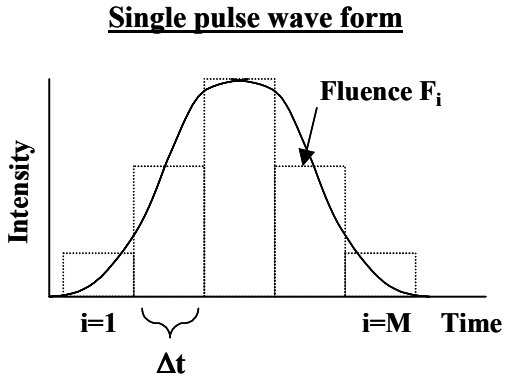

Figure 3: Gaussian temporal pulse subdivided into five flat-top sub-pulses for the finite element calculation.

2.6 Evaluating the absorption coefficients

Figure 4 shows how absorption changes in an arbitrary sample. Excited-state and two-photon absorption introduce an instantaneous jump above linear absorption for the first shot. Because excited-state absorption scales differently with

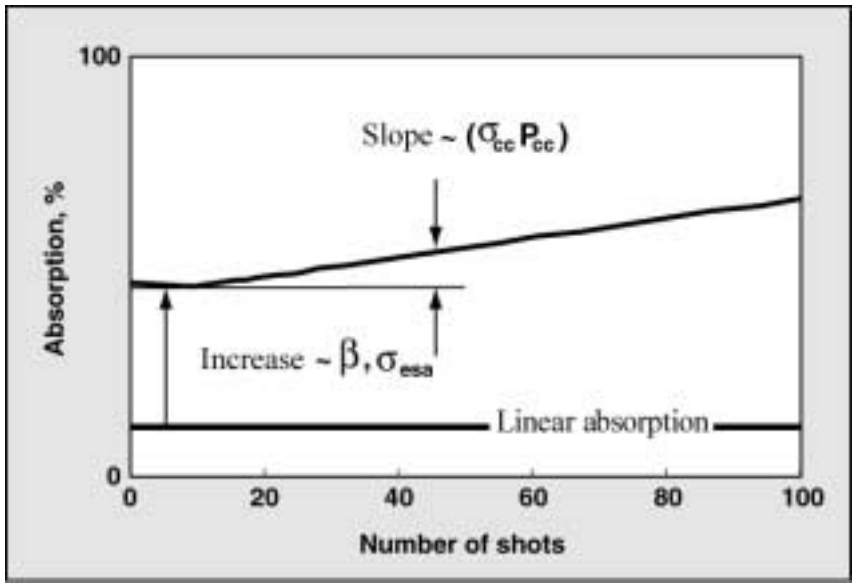

Figure 4: Effect of nonlinear absorption for small number of shots. The lower line is linear absorption and the upper curve is linear plus nonlinear absorption.

fluence than two-photon absorption, any two shots at different fluence allow the coefficients β and σ_{esa} to be directly evaluated.

Figure 4 indicates the attenuation changes slope as the number of pulses increases. Initially, the nonlinear absorption is relatively independent of the number of pulses because it is dominated by two-photon and excited-state absorption. The two-photon and excited-state absorption terms are approximately 100 times larger than the solarization term beginning with the first pulse. But as the number of pulses increases (≳20), the attenuation transitions to a linear dependence with pulses as the solarization term increases to the same order of magnitude as the two-photon and excited state terms.

3. EXPERIMENTS AND RESULTS

3.1 Experimental setup

Nonlinear absorption was induced in glass samples using the experimental setup shown in Figure 5. The setup utilizes a Q-switched, tripled-YAG laser operating at 355-nm with a pulse repetition frequency of 10 Hz. The laser has a gaussian temporal profile with a FWHM of 6.8 ns. The laser operates multi-mode and the beam at the laser's aperture has intensity variations in the form of concentric rings across its spatial profile. We focus the beam into the far-field to produce a beam at the sample that has an approximate gaussian spatial profile. The far-field focusing is accomplished using the telescope shown in Figure 5. The telescope is composed of the +2 m and –0.5 m lenses shown. The focal length of the telescope is ~20 m; hence the reason for several

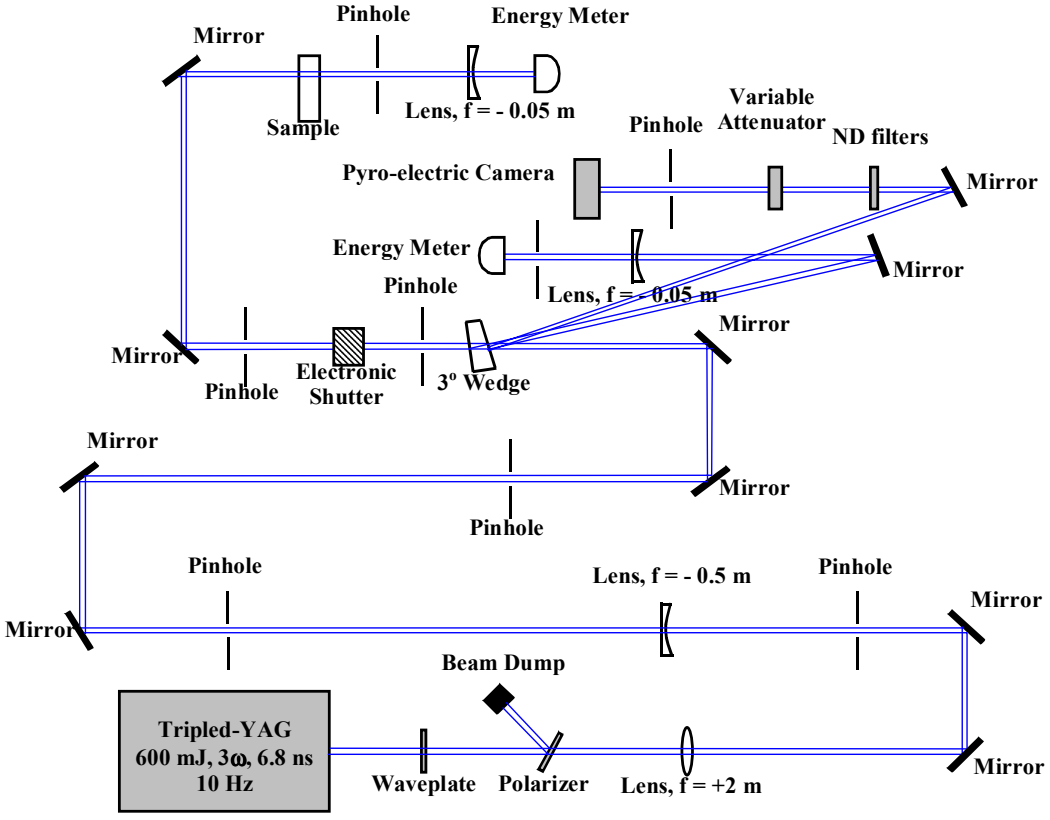

Figure 5: Experimental setup used to characterize the nonlinear absorption at 355-nm.

folding legs in the beam path. A typical beam profile measured at the sample is shown in Figure 6. The beam has a full-width at $1/e^2$ of 8 mm. The energy (fluence) incident on the sample is controlled with the waveplate and polarizer shown in Figure 5. The energy and spatial profile of the beam at the sample is measured with an energy meter and pyro-electric camera, respectively, positioned at the same distance from the 3^o wedge as the sample. A software package combined

with the camera converts the energy measurement and beam profile to a peak fluence value. Another energy meter positioned after the sample measures the transmitted energy through the sample. The transmission of the sample is then calculated by taking the ratio of $E_{transmitted}$ to $E_{incident}$. The transmission data is converted to absorption, by calculating (1 – transmission), for the analysis. The electronic shutter shown in Figure 5 is used to limit the rate pulses are incident on the sample to 1 per minute. This allows the electronics of the camera and detectors to equilibrate after each pulse and prevent the sample from heating. Fluences between 0.2 and 0.8 J/cm^2 were used in the tests with each test consisting of 100 pulses at a fixed fluence. A new site on each sample was used for each fluence test, i.e. the sample was re-positioned after a test at a given fluence.

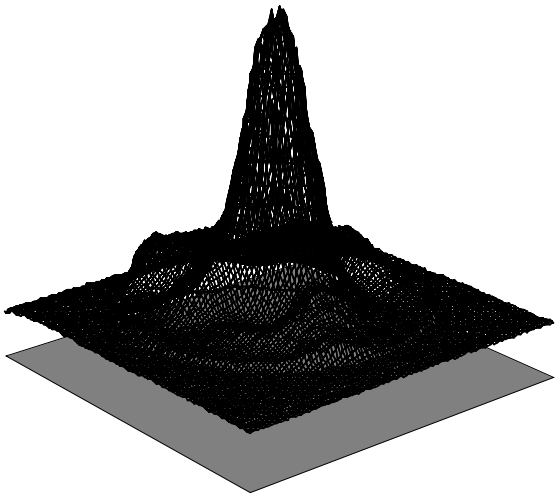

Figure 6: Spatial profile of the 355-nm, 6.8 ns YAG laser beam used for the absorption experiments. The full-width at 1/e^2 is 8 mm.

3.2 Evaluation of the absorption cross-sections

3.2.1 Absorption measurements

The absorption measurements for the BK7, UG1, and UG11 samples are shown in Figures 7, 8, and 9, respectively. The fluence used for each 100 pulse test is labeled on the plots. The scatter in the data is due to random fluctuations in the output of the laser. The fluctuations in the laser output decrease the signal-to-noise ratio at the lower fluences. In converting the transmission measurements to absorption, the index of refraction of the different glasses (inset) was used to account for the loss in transmission due to Fresnel reflections. For reference, the linear absorption is shown for each sample. The linear absorption was measured using a low-power (~5 mW) CW beam.

The first few pulses show the initial jump in absorption above linear. The remaining pulses show the solarization rate. Linear fits to the data for >20 pulses are also shown on the plots. Note the change in absorption due to solarization (>20 pulses) increases linearly as the fluence increases, as expected. Of the three glasses, UG1 shows the least propensity to solarize.

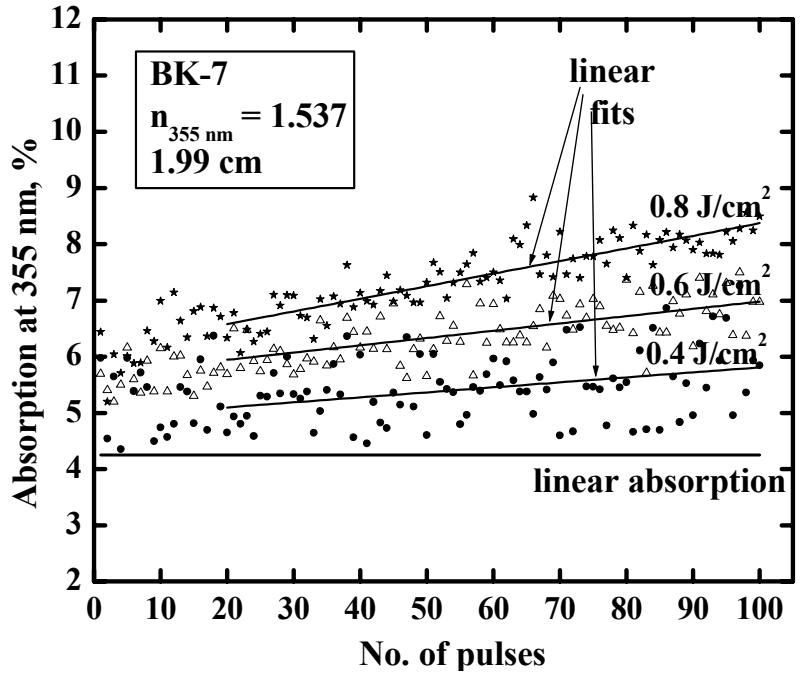

Figure 7. Absorption data for BK7. The index of refraction and thickness of the sample is given in the inset.

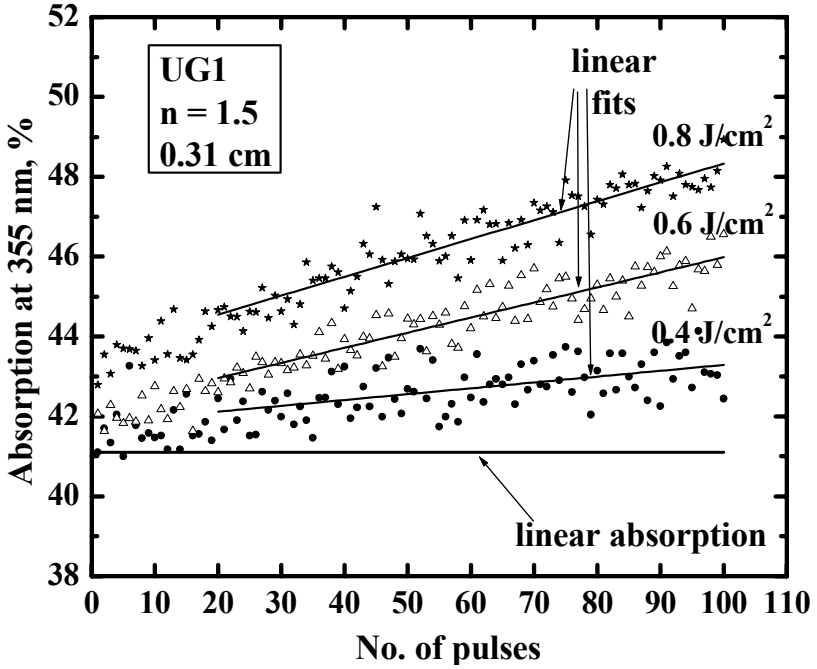

Figure 8. Absorption data for UG1. The index of refraction (estimated) and thickness of the sample is given in the inset.

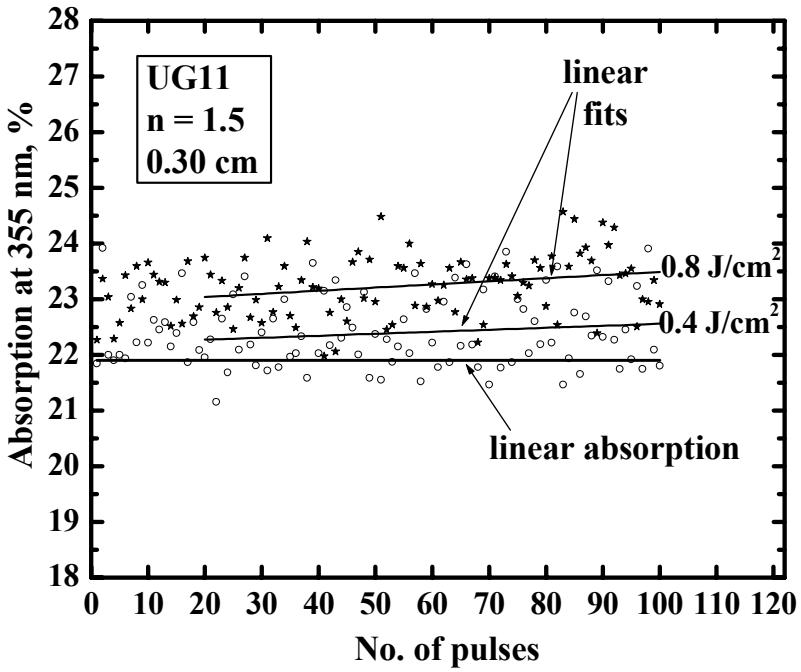

Figure 9. Absorption data for UG11. The index of refraction (estimated) and thickness of the sample is given in the inset.

3.2.2 Absorption cross-sections

Using the method discussed in section 2, solutions to equation (7) were calculated and matched to both the initial jump above linear absorption and the slope of the linear fit to the solarization. The calculated absorption was matched to the data by choosing values for the cross-sections (β, σ_{esa}, and $P_{cc}\sigma_{cc}$) that produced the closest fit. The linear fit to the data from the previous section as well as the best-fit solutions to equation (7) for BK7, UG1, and UG11 are compared in Figures 10, 11, and 12, respectively. The dashed lines in the figures show how equation (7) fits to the data using the cross-sections in Table 1. Also shown in the figures for reference is the linear absorption. Table 1 lists the coefficients that gave the closest match of the calculated absorption to the data. In general, the match between the data and calculated absorption is fair (~within 20%). The accuracy of the nonlinear coefficients is estimated to be ± 20%, and is limited by shot-to-shot data scatter. The values measured for linear absorption are within 10% of values published by the material suppliers.

Examination of the results in Table 1 reveals that the two-photon absorption cross-sections for the three glasses are comparable, with the value for UG11 being about twice that for BK7. The three glasses have relatively large magnitudes for the σ_{esa} coefficients as compared, for instance, to Cr^{3+}-doped $Na_3Ga_2Li_3F_{12}$ which has $\sigma_{esa} \sim 10^{-21}$ cm^2.[6] Of the three glasses, UG1 has the largest relative solarization coefficient ($P_{cc}\sigma_{cc}$). The material constants given in Table 1 should be regarded as specific to the particular manufacturer that these samples were procured from since historically[5] these constants have been known to vary by up to 15% between manufacturers.

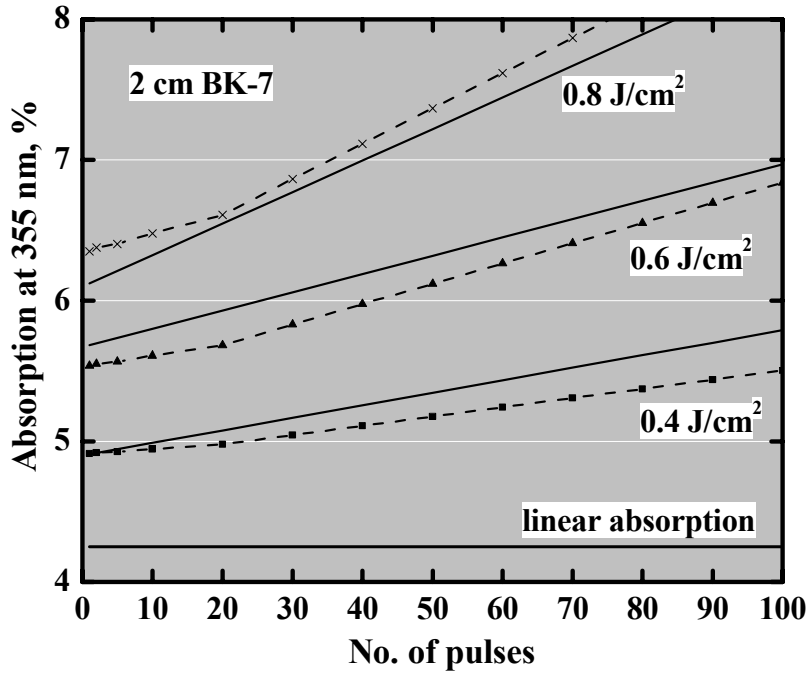

Figure 10: Fit of the calculated absorption (dashed lines) to the measured absorption (solid lines) for BK7.

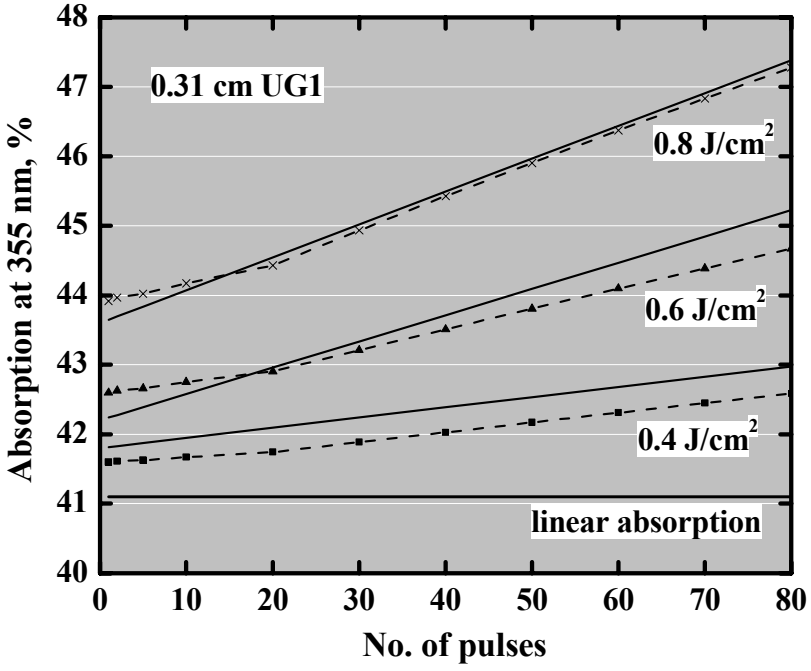

Figure 11: Fit of the calculated absorption (dashed lines) to the measured absorption (solid lines) for UG1.

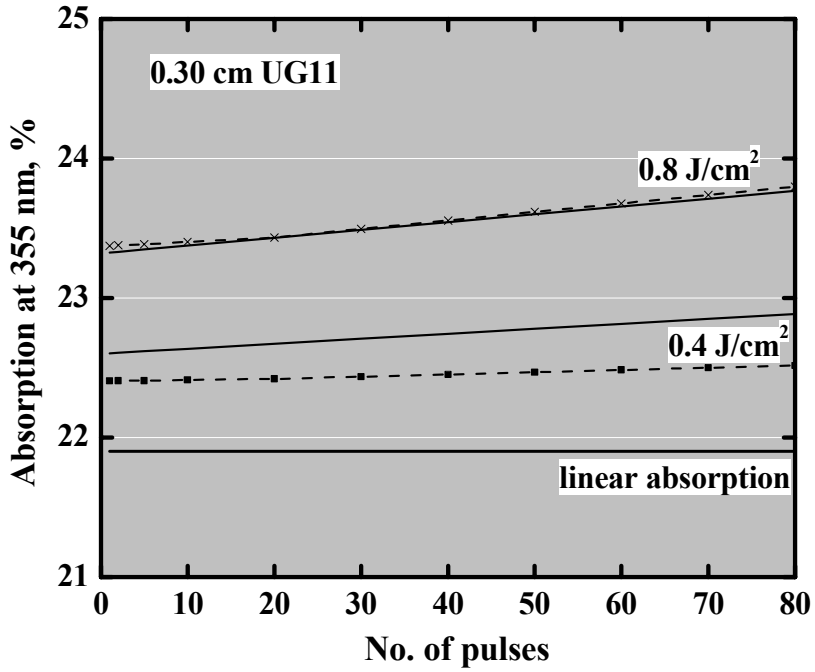

Figure 12: Fit of the calculated absorption (dashed lines) to the measured absorption (solid lines) for UG11.

	BK-7	UG1	UG11	
α	0.0217 ± 10%	1.7 ± 10%	0.82 ± 10%	cm^{-1}
β	0.025 ± 20%	0.035 ± 20%	0.047 ± 20%	$(cm\text{-}GW)^{-1}$
σ_{esa}	8.00×10^{-18} ± 20%	2.8×10^{-16} ± 20%	5×10^{-17} ± 20%	cm^2
$P_{cc}\sigma_{cc}$	8.50×10^{-20} ± 20%	2.5×10^{-18} ± 20%	1.3×10^{-19} ± 20%	cm^2

Table 1: Experimentally determined linear and nonlinear coefficients for BK7, UG1, and UG11.

3.3 Calculated transmission for 10-cm of BK7

With the linear and nonlinear coefficients in hand, the absorption equation was solved for the pulse format and glass thickness of interest for the NIF diagnostic. Figure 13 shows the effect of non-linear attenuation as a function of fluence after passing through 10-cm of BK7. The incident pulses have a constant intensity (flat-top) of 3.5 ns in this calculation.

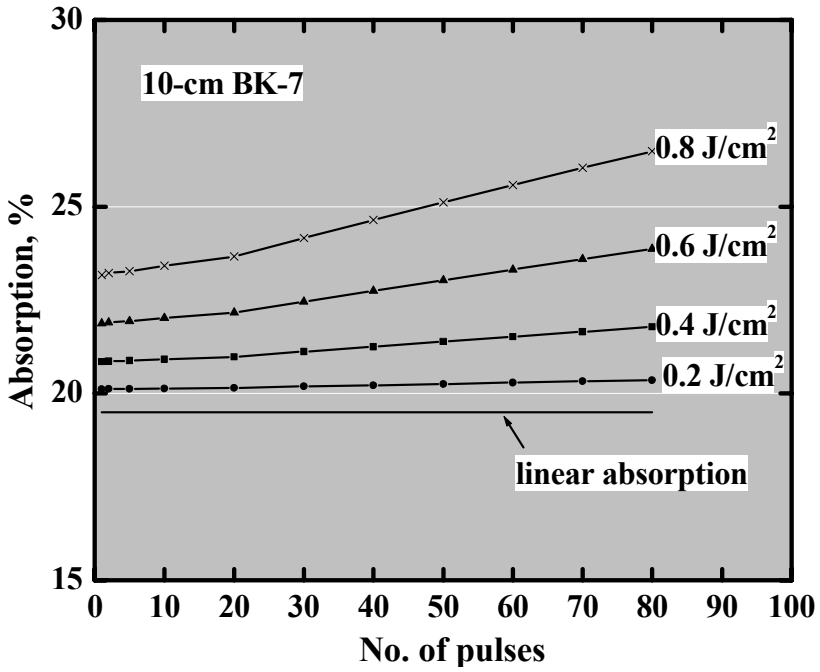

Figure 13: Calculated nonlinear absorption at 355-nm as a function of shot number in 10-cm of BK7 for several fluences using equation (7) and the coefficients listed in Table 1.

Two-photon absorption and excited-state absorption both change the temporal shape of the pulse as it passes through the sample. Two-photon absorption preferentially flattens intensity peaks, while excited-state absorption tends to absorb the pulse at its tail more than at its leading edge. Figure 14 shows the affect excited-state absorption has on a constant intensity pulse (i.e. a flat-top). There is little effect at 0.2 J/cm^2, but a 10% droop is calculated at 0.8 J/cm^2.

As can be deduced from Figures 13 and 14, nonlinear effects in 10-cm of BK7 are small (≤ 2%) for 355-nm fluences < 0.2 J/cm^2 for flat-top pulses, however, nonlinear effects are noticeable for 355-nm fluences at 0.8 J/cm^2. In particular, we see a 20% increase in the instantaneous absorption from linear, a solarization rate of 4% increase in absorption per 100 shots, and a 10% temporal droop introduced in the pulse, for 355-nm flat-top pulses at a fluence of 0.8 J/cm^2.

An attenuation calculation for 0.5-cm of UG1 absorbing glass shows the non-linear absorption has a similar effect to that from 10-cm of BK7 on the pulse shape. On the other hand, the effects in UG11 on the pulse shape are much smaller due to its smaller non-linear absorption cross-sections. The ability to calculate the effect of non-linear absorption establishes correction factors that allow determination of the true intensity and temporal profile from that detected by instruments in the NIF diagnostic.

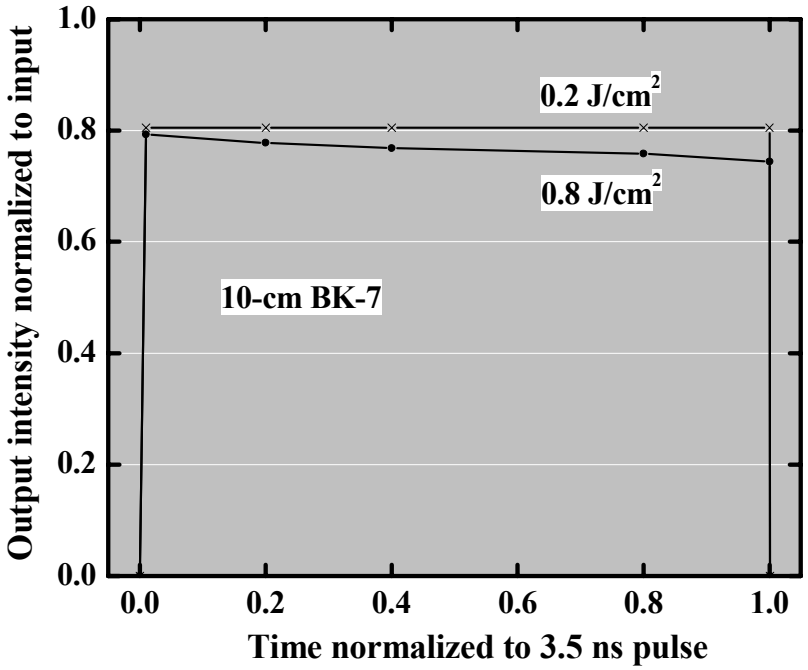

Figure 14: Pulse temporal profile upon exiting 10-cm of BK7 for a constant intensity (flat-top) input pulse.

3.4 Color center saturation

The analysis in the previous sections was based on considering nonlinear effects for only small (<100) number of pulses. However, effects for larger number of pulses (~1000) are of interest for prolonged exposure. Color center saturation has two limiting cases for a large number of pulses. Equation (4) shows the color center density saturates with an exponential dependence for large number of pulses. Furthermore, equation (5) implies the dependence may take one of two forms (cases). Case I: When the color center density n_{cc} is limited by the trap site density N_T (i.e. all the traps are populated and there is no de-trapping processes), then $n_{cc} = N_T$ at saturation regardless of the fluence per pulse. Case II: If color centers are also being destroyed by single photon absorption (i.e. de-trapping), the saturation is said to be de-trap limited. For saturation that is de-trap limited, the color center density in saturation depends on fluence as

$$\mathbf{n_{cc}(sat) = \frac{P_{cc}}{(1-P_{cc})}\frac{\beta}{2\sigma_{dt}}\int_{pulse} I^2 dt} \tag{11}$$

The two saturation cases are illustrated in Figure 15. Depending on which of these two cases apply, either N_T or σ_{dt} can be evaluated from the saturation data.

Absorption measurements where made with a large number (~10,000) of 355-nm pulses to determine which saturation limit would apply to BK7. The laser used for these measurement was a tripled-YAG laser operating at 355-nm but with a FWHM pulselength of 3.5 ns. This laser has larger pulse-to-pulse energy variations than that used to evaluate the non-linear absorption coefficients, but was more convenient for the saturation measurements because it operates at higher repetition rate. The data is shown in Figure 16. The data indicates that the saturation is primarily de-trapping limited, and corresponds to a de-trapping cross-section $\sigma_{dt} = 2\text{x}10^{-22}$ cm^2. Each absorption curve fits well to an exponential as shown. Contributions occur from a variety of color center species between the initial linear solarization regime and saturation, making it difficult to predict with any quantitative accuracy the exponential relation for these limiting cases.

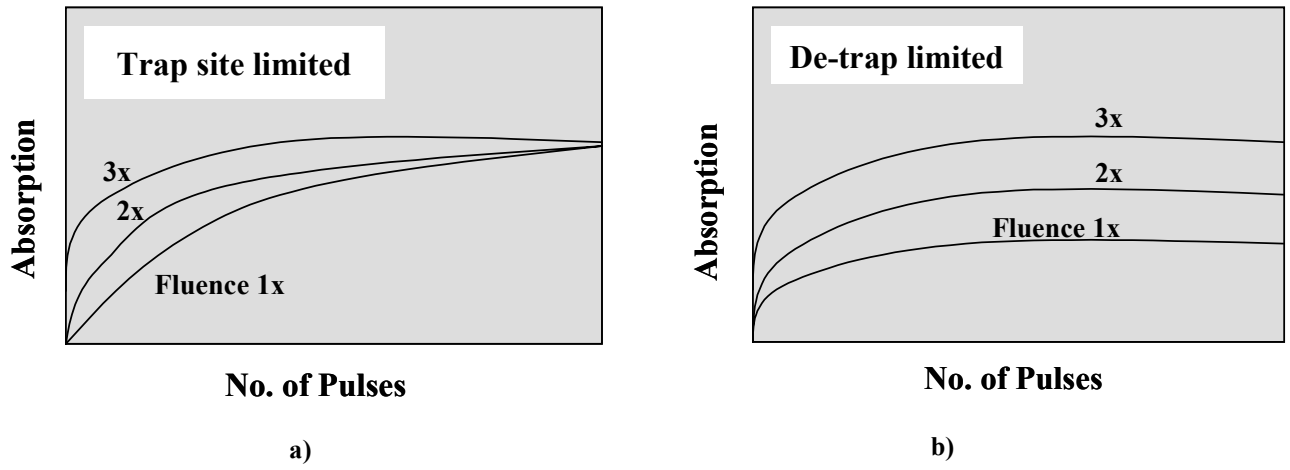

Figure 15: Illustration of nonlinear absorption saturation for large number of pulses as limited by either (a) the trap site density or (b) by color center de-trapping.

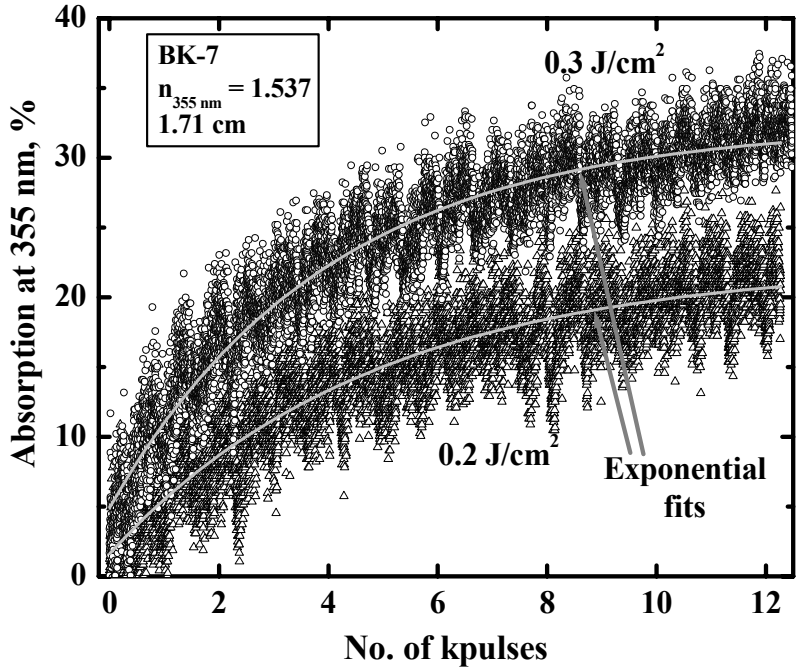

Figure 16: Solarization saturation in BK7 at two different 355-nm, 3.5 ns fluences.

4. SUMMARY

We have demonstrated a simple experimental technique that can be used to measure the nonlinear absorption coefficients in glasses. The nonlinear absorption coefficients have been determined to within 20% by first measuring the absorption induced in BK7, UG1, and UG11 on a pulse-by-pulse basis using a 355-nm laser and then evaluating the coefficients by fitting the nonlinear absorption equation to the data.

Absorption coefficients including the linear absorption coefficient α, the two-photon absorption cross-section β, the excited-state absorption cross-section σ_{esa}, and the solarization coefficient $P_{cc}\sigma_{cc}$ have been quantified for BK7, UG1, and UG11 glasses. The two-photon absorption coefficients for the three glasses are comparable with the value for UG11 being about twice that for BK7. The relative magnitudes for α and σ_{esa} for the three glasses show a consistent relation, for instance BK7 has both the lowest value for $\alpha = 0.0217 \pm 10\%$ cm^{-1} and $\sigma_{esa} = 8.0x10^{-18} \pm 20\%$ cm^2 whereas UG11 has the largest values for these coefficients, $\alpha = 0.82 \pm 10\%$ cm^{-1} and $\sigma_{esa} = 5x10^{-17} \pm 20\%$ cm^2. It was also determined that all three glasses have relatively large excited-state absorption cross-sections ($\sim 10^{-16}$-10^{-17} cm^2) as compared, for instance, to Cr^{3+}-doped $Na_3Ga_2Li_3F_{12}$ which has $\sigma_{esa} \sim 10^{-21}$ cm^2.[6] Of the three glasses, UG1 was found to have the largest relative solarization coefficient $P_{cc}\sigma_{cc} = 2.5x10^{-18} \pm 20\%$ cm^2 as compared to that found for BK7 where $P_{cc}\sigma_{cc} = 8.50x10^{-20} \pm 20\%$ cm^2. Solarization saturation in BK7 was observed to be primarily de-trapping limited with a de-trapping cross-section of $\sigma_{dt} = 2x10^{-22}$ cm^2.

For our application (FABS), nonlinear effects in 10-cm of BK7 are small ($\leq 2\%$) for 355-nm fluences <0.2 J/cm^2 for flat-top pulses, however, nonlinear effects are noticeable for 355-nm fluences at 0.8 J/cm^2. In particular, for 355-nm flat-top pulses at a fluence of 0.8 J/cm^2 we determine a 20% increase in the instantaneous absorption from linear, a solarization rate of 4% increase in absorption per 100 shots, and a 10% temporal droop introduced in the pulse.

For 0.5-cm of UG1 absorbing glass, the non-linear absorption has a similar effect as that from 10-cm of BK7 on the temporal pulse shape. On the other hand, the effects in UG11 on the pulse shape are much smaller due to its smaller non-linear absorption coefficients. The ability to calculate the effect of non-linear absorption establishes correction factors that allow determination of the true intensity and temporal profile from that detected by instruments in the NIF diagnostic.

ACKNOWLEDGEMENTS

The authors wish to thank Greg Rogowski for providing the samples used in this study and John Hollis for his assistance with the linear absorption measurements, both of LLNL. This work was performed under the auspices of the U.S. Department of Energy by the University of California, Lawrence Livermore National Laboratory under contract No. W-7405-Eng-48.

REFERENCES

1. W. L. Smith, "Two-Photon Absorption and Solarization in UV Glasses", *1982 Laser Program Annual Report*, C. Hendricks and G. Grow, eds., pp. 7-34 – 7-38, Lawrence Livermore National Laboratory, Livermore (1983)
2. L. B. Glebov, "Linear and Nonlinear Photoionization of Silicate Glasses", *Glasstech. Ber. Glass Sci. Technol.*, **75 C2**, pp. 1 - 6 (2002)
3. A. N. Trukhin, M. N. Tolstoi, L. B. Glebov, and V. L. Savelev, "Elementary Electronic Excitations in Pure Sodium Silicate Glasses", Phys. Stat. Sol. (b), **99,** 155 - 162 (1980)
4. L. B. Glebov, O. M. Efimov, G. T. Petrovskii, and P. N. Rogovtsev, "Effect of Photodecoloration on the Two-Photon Coloring of Sodium Silicate Glasses", *The Soviet Journal of Glass Physics and Chemistry*, **10**, 55 - 58 (1984)
5. C. J. Stolz, J. A. Menapace, F. Y. Genin, P. R. Ehrmann, P. E. Miller, and G. T. Rogowski, "Influence of BK7 Substrate Solarization On the Performance of Hafnia and Silica Multilayer Mirrors," in *Laser-Induced Damage in Optical Materials: 2002*, G. J. Exarhos, A. H. Guenther, N. Kaiser, K. L. Lewis, M. J. Soileau, and C. J. Stolz, eds., SPIE **4932**, 38-47 (2002)
6. J. A. Caird, S. A. Payne, P. R. Staver, A. J. Ramponi, L. L. Chase, and W. F. Krupke, "Quantum Electronic Properties of the $Na_3Ga_2Li_3F_{12}$:Cr^{3+} Laser", *IEEE J. Quantum Electron.*, **24**, 1077 – 1097 (1988)